

$\gamma\gamma \rightarrow M^+M^- (M = \pi, K)$ processes with twist-3 corrections in QCD

Cong Wang^{1,2}, Ming-Zhen Zhou^{1,a}, Hong Chen¹

¹ School of Physical Science and Technology, Southwest University, Chongqing 400715, People's Republic of China

² State Key Laboratory of Theoretical Physics, Institute of Theoretical Physics, Chinese Academy of Sciences, Beijing 100190, People's Republic of China

Received: 11 October 2016 / Accepted: 19 March 2017 / Published online: 6 April 2017
© The Author(s) 2017. This article is an open access publication

Abstract We study the $\gamma\gamma \rightarrow M^+M^- (M = \pi, K)$ processes with the contributions from the two-particle twist-2 and twist-3 distribution amplitudes of pion and kaon mesons on BHL prescription in the standard hard-scattering approach. The results show that the contributions from twist-3 parts are actually not power suppressed compared with the leading-twist contributions in the low energy region. The cross sections with twist-3 corrections agree well with the experimental data in the two-photon center-of-mass energy $W > 2.8$ GeV and we also predict the cross section ratio $\sigma_0(K^+K^-)/\sigma_0(\pi^+\pi^-)$, which is compatible with the experimental data from TPC and Belle.

1 Introduction

The common method of calculating hard exclusive processes in Quantum Chromodynamics (QCD) was developed in Refs. [1–5]. Especially, the exclusive processes at large momentum transfer have aroused much attention [3,4] in the last few years. In pioneering work, Brodsky and Lepage [4,5] put forward a systematic analysis, involving angular dependence, helicity structure, normalization of elastic and inelastic form factors and large-angle exclusive scattering amplitudes for hadrons and photons.

It is well known that the exclusive processes at large momentum transfer can afford a definite theoretical test for perturbative QCD. The two-photon processes, such as $\gamma^*\gamma \rightarrow$ hadrons and $\gamma\gamma \rightarrow$ hadron pairs at large momentum transfer, have attracted much attention in theoretical [5–10] and experimental [11–16] fields over the past few decades. Due to the pointlike structure of the photon, the initial states are simple and controllable, and the strong interactions are presented only in final states. Such a structure not only has

an important role in understanding the nonperturbative construction of QCD, but it also brings about convenience in the analysis of these exclusive hard-scattering amplitudes and perturbative mechanisms.

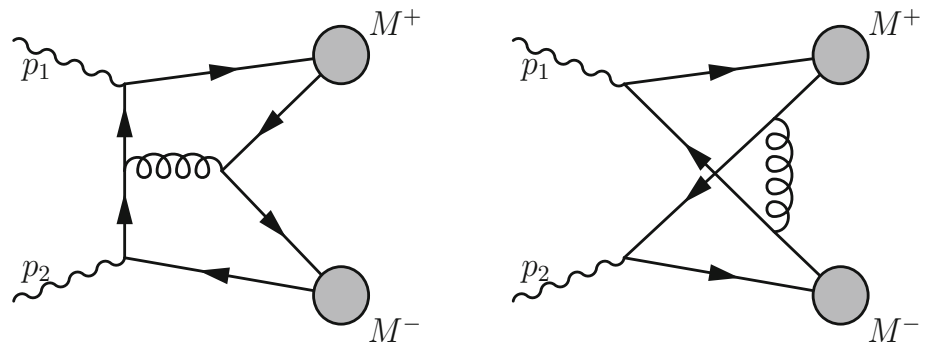
In this work, we focus on the two-photon annihilation into pseudoscalar mesons $\gamma\gamma \rightarrow M^+M^-$. However, what is troubling theorists is that the cross sections predicted in theory are noticeably below the experimental data [14]. Brodsky et al. provided the predicted results [5] as a $\sin^{-4}\theta$ dependence of the differential cross section and a W^{-6} dependence of the total cross section. Similar theoretical predictions have been put forward in Chernyak's series of works on the two-photon exclusive processes [9,10]. In 1986, Nižić [17] was the first researcher to calculate the one-loop corrections for the two-photon exclusive channels at large momentum transfer; then Goran Duplanić [18] perfected the leading-twist next-to-leading-order (NLO) radiative corrections. Their calculations indicated that the NLO corrections slightly change the leading-order predictions.

The early experimental work [11] has been suggested to test a QCD calculation in the model proposed by Brodsky and Lepage. Increasing interests in this problem, more experimental groups, for instance TPC [11], ALEPH [12], Belle [13–15] and so on have been attracted to address and present results of the theoretical analysis. Especially, the Belle Collaboration systematically measured the two-photon collisions at the center-of-mass energy $2.4 \text{ GeV} < W < 4.1 \text{ GeV}$ and the scattering-angle region $|\cos\theta| < 0.6$ [14]. This reaction will be studied with high precision at Belle-II in the near future; further theoretical research is particularly important.

Besides the QCD radiation correction [17,18], which is very minor in this process, the next-leading-order correction can also come from high Fock states or high twist distribution amplitudes of the hadron, and the latter is considered in our work. From the naive point of view, the contribu-

^a e-mail: zhoumz@swu.edu.cn

Fig. 1 Feynman diagrams for hard QCD contributions to $\gamma\gamma \rightarrow M^+M^-$



tions of high twist distribution amplitudes are suppressed by the factor $1/Q^2$ for exclusive processes with large momentum transfer Q , but that has not always been the case. For example, the contributions from twist-3 distribution amplitudes are comparable with or even larger than the one from the leading-twist distribution amplitude of light pseudoscalar meson in the $\chi_{cJ} \rightarrow \pi^+\pi^-, K^+K^-$ decay channels [19] and the pion/kaon electromagnetic form factor [20, 21]. More discussion of the high twist corrections of vector mesons is presented in Refs. [22–24]. In this work, the main experimental data of $\gamma\gamma \rightarrow M^+M^-$ processes comes from the center-of-mass energy W below 4.0 GeV and the momentum transfer is not large enough. So it is necessary to investigate the contributions from the two-particle high twist distribution amplitudes for those channels. Performing the standard calculation of the matrix element in the hard-scattering approach [5], one can easily find that the contributions from the twist-3 version are double-logarithmically divergent with the usual pion distribution amplitudes (DAs) [25, 26], which can be obtained by using a conformal expansion. Similar to the calculation of the electromagnetic form factor of the pion [27], this divergence can be removed by retaining the transverse momentum (\mathbf{k}_\perp) dependence of hard-scattering amplitude (T^{ij}) and the dangerous soft regions are suppressed by the Sudakov factor. However, the Fourier transform of the hard-scattering amplitude becomes difficult in this situation. For an estimate of the twist-3 effect, we use the Brodsky–Huang–Lepage (BHL) prescription for the harmonic-oscillator wave function (WF) [28–31] in this paper, since the BHL DAs have a better endpoint behavior in the soft regions. Our results also indicate that the twist-3 distribution amplitudes of the pion and kaon make significant contributions at the energy region $W \in (1, 6)$ GeV.

The structure of this paper is as follows. In Sect. 2, we present our calculation of the hard-scattering amplitude at tree level. A brief model of the twist-2 and twist-3 distribution amplitudes with BHL scheme is presented in Sect. 3. Section 4 is the numerical analysis and the last section is the conclusion to this work. The hard-scattering amplitudes for $\gamma\gamma \rightarrow \pi^+\pi^-, K^+K^-$ are given in Appendix A.

2 Calculation of hard-scattering amplitudes

In this section, we want to recalculate the hard-scattering amplitudes for

$$\gamma_1(p_1, \varepsilon_1^{\lambda_1}) + \gamma_2(p_2, \varepsilon_2^{\lambda_2}) \rightarrow M^+(p_3) + M^-(p_4), \quad (1)$$

$$(M = \pi, K)$$

where the initial photons are real with the different polarization and the final states are flavor-nonsinglet helicity-zero mesons. p_1, p_2 and p_3, p_4 are four-momenta for the initial photons and the final pseudoscalar mesons, respectively. $\varepsilon_1^{\lambda_1}(\varepsilon_2^{\lambda_2})$ are the photons' polarization and the $\lambda_1(\lambda_2) = \pm 1$ represent two transversal photons. This process is described by the $\gamma\gamma \rightarrow (q\bar{q}) + (q\bar{q})$ amplitude which is illustrated by two typical lowest order Feynman diagrams in Fig. 1. The other 18 diagrams, which can be obtained by exchanging the photons, gluons and quark lines, are not shown in the paper.

In the two-photon center-of-mass frame, we choose the direction of two-photon collision as the Z-axis with the total energy denoted by W and the scattering angle denoted by θ . The four-momenta of incoming and outgoing particles are given as follows:

$$p_1 = \frac{W}{2}(1, 0, 0, 1), \quad p_2 = \frac{W}{2}(1, 0, 0, -1),$$

$$p_3 = \frac{W}{2}(1, \sin \theta, 0, \cos \theta),$$

$$p_4 = \frac{W}{2}(1, -\sin \theta, 0, -\cos \theta), \quad (2)$$

where the masses of pion and kaon are vanish in the chiral limit. The polarization states of the photons are taken to be

$$\varepsilon_1^+(p_1) = \frac{1}{\sqrt{2}}(0, -1, -i, 0), \quad \varepsilon_1^-(p_1) = \frac{1}{\sqrt{2}}(0, 1, -i, 0),$$

$$\varepsilon_2^+(p_2) = \frac{1}{\sqrt{2}}(0, 1, -i, 0), \quad \varepsilon_2^-(p_2) = \frac{1}{\sqrt{2}}(0, -1, -i, 0). \quad (3)$$

With the above choices, we work out the expression of cross section with the two-particle twist-3 distribution ampli-

tudes of the final pion mesons in the hard-scattering approach [5] and it is written as

$$\frac{d\sigma(\gamma\gamma \rightarrow \pi^+\pi^-)}{d\cos\theta} = \frac{1}{32\pi W^2} \frac{1}{4} \sum_{\lambda_1, \lambda_2=\pm 1} |A_{\lambda_1\lambda_2}|^2, \quad (4)$$

$$A_{\lambda_1\lambda_2}(W, \theta) = \int_0^1 \int_0^1 dx dy \sum_{ij} \phi_\pi^i(x, \mu_F^2) \times T_{\lambda_1\lambda_2}^{ij}(x, y, W, \theta) \phi_\pi^j(y, \mu_F^2), \quad (5)$$

where $A_{\lambda_1\lambda_2}$ is the transitional matrix element of the two-photon scattering process. $\phi_\pi^i(x, \mu_F^2)$ is the pion meson distribution amplitude with the longitudinal momentum fraction x and the factorization scale μ_F . The notation $i = \pi$ represents the twist-2 distribution amplitude and the notation $i = p, \sigma$ represents the two twist-3 distribution amplitudes. The function $T_{\lambda_1\lambda_2}^{ij}(x, y, W, \theta)$ is the hard-scattering amplitude from the different distribution amplitudes with the notation i and j .

To calculate the transitional matrix element, we take the vacuum saturation approximation and use the Fierz identity,

$$\begin{aligned} \bar{q}_1 \alpha q_2 \beta &= \frac{1}{4} I_{\beta\alpha} (\bar{q}_1 q_2) - \frac{1}{4} (i\gamma_5)_{\beta\alpha} (\bar{q}_1 i\gamma^5 q_2) \\ &+ \frac{1}{4} (\gamma_\mu)_{\beta\alpha} (\bar{q}_1 \gamma^\mu q_2) - \frac{1}{4} (\gamma_\mu \gamma_5)_{\beta\alpha} (\bar{q}_1 \gamma^\mu \gamma^5 q_2) \\ &+ \frac{1}{8} (\sigma_{\mu\nu} \gamma_5)_{\beta\alpha} (\bar{q}_1 \sigma^{\mu\nu} \gamma^5 q_2), \end{aligned} \quad (6)$$

where q_1 and q_2 are the quark fields. There are only three terms with the matrix γ_5 that have contributions for scattering amplitudes in the $\gamma\gamma \rightarrow \pi^+\pi^-$ process by the parity analysis. Finally, we find have the notation with nonvanishing terms $ij = \pi\pi, pp, p\sigma, \sigma p, \sigma\sigma$ for the hard-scattering amplitude $T_{\lambda_1\lambda_2}^{ij}(x, y, W, \theta)$ of this reaction. The twist-2 and twist-3 distribution amplitudes of the pion are defined as the following relations:

$$\begin{aligned} \langle \pi^+(p) | \bar{u}(z_1) \gamma^\mu \gamma^5 d(z_2) | 0 \rangle \\ = -if_\pi p^\mu \int_0^1 dx e^{i(x \cdot p \cdot z_1 + (1-x) \cdot p \cdot z_2)} \phi_\pi^\pi(x), \end{aligned} \quad (7)$$

$$\begin{aligned} \langle \pi^+(p) | \bar{u}(z_1) i\gamma^5 d(z_2) | 0 \rangle \\ = f_\pi \mu_\pi \int_0^1 dx e^{i(x \cdot p \cdot z_1 + (1-x) \cdot p \cdot z_2)} \phi_\pi^p(x), \end{aligned} \quad (8)$$

$$\begin{aligned} \langle \pi^+(p) | \bar{u}(z_1) \sigma^{\mu\nu} \gamma^5 d(z_2) | 0 \rangle \\ = \frac{if_\pi \mu_\pi}{6} [p^\mu (z_1 - z_2)^\nu - p^\nu (z_1 - z_2)^\mu] \\ \times \int_0^1 dx e^{i(x \cdot p \cdot z_1 + (1-x) \cdot p \cdot z_2)} \phi_\pi^\sigma(x), \end{aligned} \quad (9)$$

by the expanded form of hadronic matrix element [25, 32–34], where f_π is the decay constant of pion, the parameter

$\mu_\pi = \frac{m_\pi^2}{m_u + m_d}$ is proportional to the chiral condensate and the variable x is the meson momentum fraction.

With the definitions of distribution amplitudes for final state mesons, the transitional matrix element of the $\gamma\gamma \rightarrow \pi^+\pi^-$ process is calculated and the hard-scattering amplitude $T_{\lambda_1\lambda_2}^{ij}(x, y, W, \theta)$ is represented as

$$T_{\lambda_1\lambda_2}^{ij}(x, y, W, \theta) = \frac{16}{3} \pi^2 \alpha \alpha_s (\mu_R^2) C_F \hat{T}_{\lambda_1\lambda_2}^{ij} \frac{1}{l_1^2 l_2^2 l_3^2}, \quad (10)$$

where $C_F = \frac{4}{3}$ is the color factor and the masses of the light quarks are neglected. α is the electromagnetic coupling constant and $\alpha_s(\mu_R^2)$ is the strong coupling constant with the renormalization scale μ_R . The operator $\hat{T}_{\lambda_1\lambda_2}^{ij}$ is related to the two-pion materialization of two photons with different twist distribution amplitudes and has diverse expressions from the various Feynman diagrams. For instance, it is given as

$$\begin{aligned} \hat{T}_{\lambda_1\lambda_2}^{\pi\pi} &= \frac{1}{16} f_\pi^2 \text{Tr}[\not{\epsilon}_1 \not{l}_1 \gamma_\rho \not{l}_2 \not{\epsilon}_2 \gamma_5 \not{p}_4 \gamma^\rho \gamma_5 \not{p}_3], \\ \hat{T}_{\lambda_1\lambda_2}^{pp} &= \frac{1}{16} f_\pi^2 \mu_\pi^2 \text{Tr}[\not{\epsilon}_1 \not{l}_1 \gamma_\rho \not{l}_2 \not{\epsilon}_2 \gamma_5 \gamma^\rho \gamma_5], \\ \hat{T}_{\lambda_1\lambda_2}^{p\sigma} &= -\frac{1}{96} f_\pi^2 \mu_\pi^2 p_3^\alpha \left(\frac{\partial}{\partial l_{1\beta}} - \frac{\partial}{\partial l_{3\beta}} \right) \\ &\times \text{Tr}[\not{\epsilon}_1 \not{l}_1 \gamma_\rho \not{l}_2 \not{\epsilon}_2 \gamma_5 \gamma^\rho \gamma_5 \sigma_{\alpha\beta}], \\ \hat{T}_{\lambda_1\lambda_2}^{\sigma p} &= -\frac{1}{96} f_\pi^2 \mu_\pi^2 p_4^\mu \left(\frac{\partial}{\partial l_{3\nu}} - \frac{\partial}{\partial l_{2\nu}} \right) \\ &\times \text{Tr}[\not{\epsilon}_1 \not{l}_1 \gamma_\rho \not{l}_2 \not{\epsilon}_2 \gamma_5 \sigma_{\mu\nu} \gamma^\rho \gamma_5], \\ \hat{T}_{\lambda_1\lambda_2}^{\sigma\sigma} &= \frac{1}{576} f_\pi^2 \mu_\pi^2 p_3^\alpha \left(\frac{\partial}{\partial l_{1\beta}} - \frac{\partial}{\partial l_{3\beta}} \right) p_4^\mu \left(\frac{\partial}{\partial l_{3\nu}} - \frac{\partial}{\partial l_{2\nu}} \right) \\ &\times \text{Tr}[\not{\epsilon}_1 \not{l}_1 \gamma_\rho \not{l}_2 \not{\epsilon}_2 \gamma_5 \sigma_{\alpha\beta} \gamma^\rho \gamma_5 \sigma_{\mu\nu}], \end{aligned} \quad (11)$$

in the left diagram of Fig. 1, where ϵ_1 and ϵ_2 are abbreviations of the polarizations $\epsilon_1^{\lambda_1}(p_1)$ and $\epsilon_2^{\lambda_2}(p_2)$ of the initial photons, respectively. The partial $(\frac{\partial}{\partial l_{m\nu}} - \frac{\partial}{\partial l_{n\nu}})$ ($m, n = 1, 2, 3$) comes from the $(z_1 - z_2)^\nu$ of Eq. (9). The momenta of the quark propagators are represented by l_1, l_2 and the gluon propagator is represented by l_3 . In this diagram, they can be expressed in terms of the external momenta $l_1 = -p_1 + (1-x)p_3$, $l_2 = p_2 - yp_4$ and $l_3 = -xp_3 - (1-y)p_4$. Finally, we obtain the hard-scattering amplitudes $T_{\lambda_1\lambda_2}^{ij}(x, y, W, \theta)$ with the notation $ij = \pi\pi, pp, p\sigma, \sigma p, \sigma\sigma$ by the sum of 20 Feynman diagrams and their detailed expressions are shown in Appendix A. One can find that the twist-2 part ($T_{\lambda_1\lambda_2}^{\pi\pi}$) is proportional to $\frac{1}{W^2}$, and the twist-3 part ($T_{\lambda_1\lambda_2}^{pp}, T_{\lambda_1\lambda_2}^{p\sigma}, T_{\lambda_1\lambda_2}^{\sigma p}, T_{\lambda_1\lambda_2}^{\sigma\sigma}$) is proportional to $\frac{1}{W^4}$. Compared with the twist-2 part, the twist-3 part is obviously suppressed by a factor $\frac{1}{W^2}$.

3 The distribution amplitudes of pseudoscalar mesons

The twist-2 and twist-3 distribution amplitudes of pseudoscalar mesons are taken as the main nonperturbative input parameters in the above calculations of hard-scattering amplitude. In this section, we give a brief review for them in the BHL scheme [29–31]. One useful way of modeling the hadronic WF is to use the approximate bound-state solution of a hadron in terms of the quark model. We take the simplest possible model, viz., the harmonic-oscillator model. The BHL prescription of the WF is correctly obtained by connecting the equal time WF in the rest frame and the WF in the infinite momentum frame. This particular \mathbf{k}_\perp -dependence goes along with a factor $\exp[-\frac{1}{\beta^2}(\frac{m_q^2}{x} + \frac{m_{\bar{q}}^2}{1-x})]$ in the harmonic-oscillator WF, i.e., the BHL WFs $\Psi(x, \mathbf{k}_\perp)$ can be obtained by the replacement

$$\frac{\mathbf{k}_\perp^2}{x(1-x)} \rightarrow \frac{\mathbf{k}_\perp^2}{x(1-x)} + \frac{m_q^2}{x} + \frac{m_{\bar{q}}^2}{1-x}. \quad (12)$$

Here, the quark masses m_q and $m_{\bar{q}}$ are effective quark masses from the renormalization due to the reduction of higher Fock states as functionals of the valence state [35], not current quark masses, i.e., the quark masses appearing in the QCD Lagrangian. In Ref. [36], Brodsky showed the effective light quark masses $m_u = m_d = 46$ MeV, $m_s = 357$ MeV by fitting the quark masses to the observed masses of the π and K . In Refs. [37, 38], the authors consider two cases, the values for the effective quark masses are fixed at a typical current one and a typical constituent one, respectively. As suggested above, the BHL WFs of the pseudoscalar meson can be written as

$$\Psi(x, \mathbf{k}_\perp) \propto \exp\left[-\frac{1}{8\beta^2}\left(\frac{\mathbf{k}_\perp^2 + m_1^2}{x} + \frac{\mathbf{k}_\perp^2 + m_2^2}{1-x}\right)\right] \quad (13)$$

from the harmonic-oscillator model at the rest frame. As the input parameters for the DAs, the effective quark masses m_i ($i = 1, 2$) play an important role as model parameters. In our paper, they are scale independent and we hold them to be the typical constituent quark masses.

The β refers to the harmonic parameter, which can be obtained from the definition of the average of the quark transverse momentum squared,

$$\langle \mathbf{k}_\perp^2 \rangle_M = \frac{f_M^2}{24} \int dx \frac{d^2 \mathbf{k}_\perp}{16\pi^3} |\mathbf{k}_\perp|^2 |\Psi_M(x, \mathbf{k}_\perp)|^2 / P_{q\bar{q}}^M, \quad (14)$$

where $M = \pi$ for pion and $M = K$ for kaon mean the leading-twist wave functions Ψ_π^π and Ψ_K^K . The decay constants are $f_\pi = 0.132$ GeV for pion and $f_K = 0.160$ GeV for kaon, respectively. In Refs. [29–31], $\langle \mathbf{k}_\perp^2 \rangle_\pi$ and $\langle \mathbf{k}_\perp^2 \rangle_K$ are all given as $(0.356 \text{ GeV})^2$ approximately. The probability of finding the $q\bar{q}$ leading-twist Fock state in the pseudoscalar meson is not larger than unity,

$$P_{q\bar{q}}^M = \frac{f_M^2}{24} \int dx \frac{d^2 \mathbf{k}_\perp}{16\pi^3} |\Psi_M(x, \mathbf{k}_\perp)|^2 \leq 1. \quad (15)$$

The classical forms of the twist-2 and twist-3 wave functions with BHL prescription are widely considered and have the immediate advantage to solve the endpoint singularity by the exponential suppression in the $x = 0$ and $x = 1$ points. In our work, we take the twist-2 wave functions of pion and kaon with the first three terms of the Gegenbauer polynomials and they are characterized as

$$\begin{aligned} \Psi_\pi^\pi(x, \mathbf{k}_\perp) &= A_\pi^\pi \left[1 + B_\pi^\pi C_2^{\frac{3}{2}}(\xi) + C_\pi^\pi C_4^{\frac{3}{2}}(\xi) \right] \\ &\times \exp\left[-\frac{\mathbf{k}_\perp^2 + m_q^2}{8\beta_\pi^2 x(1-x)}\right], \end{aligned} \quad (16)$$

$$\begin{aligned} \Psi_K^K(x, \mathbf{k}_\perp) &= A_K^K \left[1 + B_K^K C_1^{\frac{3}{2}}(\xi) + C_K^K C_2^{\frac{3}{2}}(\xi) \right] \\ &\times \exp\left[-\frac{1}{8\beta_K^2} \left(\frac{\mathbf{k}_\perp^2 + m_q^2}{x} + \frac{\mathbf{k}_\perp^2 + m_s^2}{1-x} \right)\right], \end{aligned} \quad (17)$$

where $C_n^{\frac{3}{2}}(\xi)$ is associated with the Gegenbauer polynomials; we have the relationship $\xi = 2x - 1$ and we take $n = 2, 4$ in the pion case for the $SU(2)$ isotopic symmetry and $n = 1, 2$ in the kaon case for the $SU(3)$ -flavor symmetry breaking. The constituent quark masses $m_q = 0.30$ GeV ($q = u, d$) and $m_s = 0.45$ GeV [19] are given in the above formulas. To simplify the following numerical analysis, we write the twist-3 wave functions as

$$\Psi_\pi^p(x, \mathbf{k}_\perp) = \frac{A_\pi^p}{x(1-x)} \exp\left[-\frac{\mathbf{k}_\perp^2 + m_q^2}{8\beta_\pi^2 x(1-x)}\right], \quad (18)$$

$$\Psi_\pi^\sigma(x, \mathbf{k}_\perp) = A_\pi^\sigma \exp\left[-\frac{\mathbf{k}_\perp^2 + m_q^2}{8\beta_\pi^2 x(1-x)}\right], \quad (19)$$

and

$$\begin{aligned} \Psi_K^p(x, \mathbf{k}_\perp) &= \frac{A_K^p}{x(1-x)} \exp\left[-\frac{1}{8\beta_K^2} \left(\frac{\mathbf{k}_\perp^2 + m_q^2}{x} + \frac{\mathbf{k}_\perp^2 + m_s^2}{1-x} \right)\right], \end{aligned} \quad (20)$$

$$\Psi_K^\sigma(x, \mathbf{k}_\perp) = A_K^\sigma \exp\left[-\frac{1}{8\beta_K^2} \left(\frac{\mathbf{k}_\perp^2 + m_q^2}{x} + \frac{\mathbf{k}_\perp^2 + m_s^2}{1-x} \right)\right], \quad (21)$$

for the pion and kaon, respectively.

The above wave functions of twist-2 and twist-3 for pion and kaon follow the normalization condition,

$$\int dx \frac{d^2 \mathbf{k}_\perp}{16\pi^3} \Psi_M^i(x, \mathbf{k}_\perp) = 1, \quad (22)$$

where the notation $i = \pi(K), p, \sigma$ refers to the different twist wave functions and the symbol $M = \pi(K)$ refers to the

pion (kaon) meson. By integrating the transverse momentum of the wave function, the corresponding distribution amplitude is acquired from the relationship

$$\phi_M^i(x, \mu_F^2) = \int_{|\mathbf{k}_\perp| < \mu_F} \frac{d^2\mathbf{k}_\perp}{16\pi^3} \Psi_M^i(x, \mathbf{k}_\perp), \quad (23)$$

where μ_F is the upper limit of integral which refers to the ultraviolet cutoff. In order to simplify the following calculation, one can safely take $\mu_F \rightarrow +\infty$ due to the smallness of the wave function in the region of $|\mathbf{k}_\perp| > \mu_F$. Substituting Eqs. (16)–(21) into Eq. (23), we obtain the meson distribution amplitudes

$$\begin{aligned} \phi_\pi^\pi(x) &= \frac{A_\pi^\pi \beta_\pi^2}{2\pi^2} x(1-x) [1 + B_\pi^\pi C_2^{\frac{3}{2}}(\xi) + C_\pi^\pi C_4^{\frac{3}{2}}(\xi)] \\ &\times \exp\left[-\frac{m_q^2}{8\beta_\pi^2 x(1-x)}\right], \end{aligned} \quad (24)$$

$$\phi_\pi^p(x) = \frac{A_\pi^p \beta_\pi^2}{2\pi^2} \exp\left[-\frac{m_q^2}{8\beta_\pi^2 x(1-x)}\right], \quad (25)$$

$$\phi_\pi^\sigma(x) = \frac{A_\pi^\sigma \beta_\pi^2}{2\pi^2} x(1-x) \exp\left[-\frac{m_q^2}{8\beta_\pi^2 x(1-x)}\right] \quad (26)$$

for the pion and

$$\begin{aligned} \phi_K^K(x) &= \frac{A_K^K \beta_K^2}{2\pi^2} x(1-x) [1 + B_K^K C_1^{\frac{3}{2}}(\xi) + C_K^K C_2^{\frac{3}{2}}(\xi)] \\ &\times \exp\left[-\frac{(1-x)m_q^2 + xm_s^2}{8\beta_K^2 x(1-x)}\right], \end{aligned} \quad (27)$$

$$\phi_K^p(x) = \frac{A_K^p \beta_K^2}{2\pi^2} \exp\left[-\frac{(1-x)m_q^2 + xm_s^2}{8\beta_K^2 x(1-x)}\right], \quad (28)$$

$$\phi_K^\sigma(x) = \frac{A_K^\sigma \beta_K^2}{2\pi^2} x(1-x) \exp\left[-\frac{(1-x)m_q^2 + xm_s^2}{8\beta_K^2 x(1-x)}\right], \quad (29)$$

for the kaon, respectively. The above coefficients A_M^i , B_M^i , C_M^i , A_M^p , A_M^σ and the harmonic parameters β_M are worked out in the following discussion.

With the method of nonlocal operator product expansion and conformal symmetry, the distribution amplitudes of the pion [26] and kaon [39] have been studied and the general form of the leading-twist distribution amplitude with the expansion of Gegenbauer polynomials were described as

$$\phi_M^i(x, \mu_F^2) = 6x(1-x) \left(1 + \sum_{n=1}^{\infty} a_n^i(\mu_F^2) C_n^{\frac{3}{2}}(2x-1)\right). \quad (30)$$

To leading logarithmic accuracy, the coefficients of non-perturbative Gegenbauer polynomials a_n^i renormalize multiplicatively with

$$a_n^i(\mu_F^2) = L^{\frac{\gamma_n^{(0)}}{\beta_0}} a_n^i(\mu_0^2), \quad (31)$$

where $L = \frac{\alpha_s(\mu_F^2)}{\alpha_s(\mu_0^2)}$, $\beta_0 = \frac{11N_c - 2N_f}{3}$. The quantity n takes even values for the pion and positive integers for the kaon. The anomalous dimension $\gamma_n^{(0)}$ can be expressed as

$$\gamma_n^{(0)} = 4C_F \left(\psi(n+2) + \gamma_E - \frac{3}{4} - \frac{1}{2(n+1)(n+2)} \right). \quad (32)$$

Those coefficients a_n^i of the Gegenbauer polynomials were mainly calculated by QCD sum rules [26, 39–41]. Their values are

$$\begin{aligned} a_2^\pi(1 \text{ GeV}) &= 0.25 \pm 0.15, & a_4^\pi(1 \text{ GeV}) &= 0.04 \pm 0.11, \\ a_1^K(1 \text{ GeV}) &= 0.06 \pm 0.03, & a_2^K(1 \text{ GeV}) &= 0.25 \pm 0.15. \end{aligned} \quad (33)$$

Additionally, the recent values of the coefficient $a_2(\mu = 2 \text{ GeV})$ obtained from lattice QCD [42–44] are within the range that we adopted in our calculation.

The moments of the leading-twist distribution amplitudes are defined by the following expression:

$$\langle \xi^n \rangle_M^i = \int_0^1 (2x-1)^n \phi_M^i(x) dx. \quad (34)$$

Here the scripts $n = 0, 2, 4$ and $n = 0, 1, 2$ are the first three moments for the pion and kaon meson, respectively. In this formula, the form of the distribution amplitude $\phi_M^i(x)$ is taken as our BHL scheme Eqs. (24) and (27) and the general form Eq. (30). Equating the two sets of moments and taking the constraint $\langle \mathbf{k}_\perp^2 \rangle_\pi \approx \langle \mathbf{k}_\perp^2 \rangle_K \approx (0.356 \text{ GeV})^2$, we figure out the harmonic parameters $\beta_{\pi, K}$ and the twist-2 Gegenbauer coefficients A_M^i , B_M^i , C_M^i ($i = \pi, K$; $M = \pi, K$). The coefficients A_π^p , A_π^σ and A_K^p , A_K^σ of the twist-3 distribution amplitudes can be directly worked out by the normalized condition Eq. (22). Substituting Eq. (33) into the previous discussion, the parameters of the distribution amplitudes and the probability of finding the $q\bar{q}$ leading-twist Fock state in the pion or kaon are listed in Table 1 with the scale value $\mu_F = 1 \text{ GeV}$. The deviation of those parameters comes from uncertainties of the twist-2 Gegenbauer coefficients in Eq. (33). We find that $P_{q\bar{q}}^\pi \leq 0.27$ and $P_{q\bar{q}}^K \leq 0.5$ are much smaller than unity. So higher twist and higher Fock states are also important components for the pion and kaon, which need to be taken into account in our work. In the above analysis, we only get the coefficients of the distribution amplitudes in the BHL scheme with the initial value $\mu_F = 1 \text{ GeV}$. Then we take the scale value $\mu_F^2 = W^2$. According to the QCD evolution of the coefficients Eq. (31) and substituting Eq. (33) into Eq. (31), we can obtain the BHL distribution amplitudes with any scale value W using the previous method. The evolution method we adopt in our paper is equivalent to the famous evo-

Table 1 The parameters of twist-2,3 distribution amplitudes for the pion and kaon mesons in Eqs. (27)–(29) with the scale value $\mu_F = 1$ GeV. The dimensions of the harmonic parameters $\beta_{\pi,K}$ and normal-

ization coefficients A_M^i ($i = \pi, K, p, \sigma; M = \pi, K$) are GeV and $(\text{GeV})^{-2}$, respectively. The others parameters are dimensionless

β_π	$P_{q\bar{q}}^\pi$	A_π^π	B_π^π	C_π^π	A_π^p	A_π^σ
0.47 ± 0.05	0.26 ± 0.01	851.1 ± 181.4	0.47 ± 0.21	0.19 ± 0.17	145.3 ± 39.0	768.8 ± 197.1
β_K	$P_{q\bar{q}}^K$	A_K^K	B_K^K	C_K^K	A_K^p	A_K^σ
0.44 ± 0.02	0.44 ± 0.05	1226.3 ± 121.0	0.21 ± 0.04	0.47 ± 0.15	200.6 ± 30.0	1031.5 ± 148.1

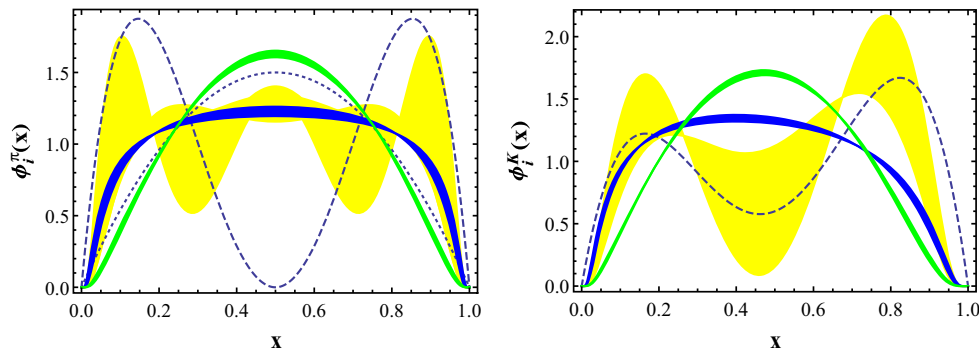


Fig. 2 The characteristic shapes of the distribution amplitudes for pion and kaon in BHL frame with the scale value $W \in (1, 6)$ GeV. *Left panel:* Yellow band ϕ_π^π ; Blue band ϕ_π^p ; Green band ϕ_π^σ . Dashed line the CZ distribution amplitude, $\phi_\pi^{CZ}(x) = 30x_d x_u (x_d - x_u)^2$, dotted line the

asymptotic distribution amplitude, $\phi_\pi^{asy}(x) = 6x(1-x)$. *Right panel:* Same for ϕ_K^i ; $\phi_K^{CZ}(x) = 30x_s x_u [0.6(x_s - x_u)^2 + 0.08 + 0.08(x_s - x_u)]$

lution equation (2.17a) in Ref. [4]. A similar discussion as regards this evolution method can be found in Refs. [45,46].

In Fig. 2, the twist-2 and twist-3 distribution amplitudes for the pion and kaon of the BHL scheme are illustrated with the variable scale $W \in (1, 6)$ GeV. As can be seen from Fig. 2, the distribution amplitudes in the BHL prescription are obviously different from the common forms in the points $x = 0$ and 1. The endpoint singularities coming from the hard-scattering amplitudes are suppressed by the effective endpoint behavior. The banded graphics of the distribution amplitudes mean the uncertainties of the parameters, which come from the strong coupling constant α_s with $\Lambda_{QCD} \in (0.15, 0.3)$ GeV, the center-of-mass energy $W \in (1, 6)$ GeV and the Gegenbauer coefficients a_n^i from Eq. (33). Especially, the area of the pion ϕ_π^π is more complicated than the one of the kaon ϕ_K^K , since we take the Gegenbauer polynomials to the $C_4^{\frac{3}{2}}$ term with the coefficient a_4^π changing from positive value to negative value for the pion, but the coefficient a_2^K is always positive for the kaon. The graphics of the twist-3 distribution amplitudes without Gegenbauer polynomials are simple for the pion and kaon.

4 Numerical analysis

To analyze the scattering cross section of two-photon annihilation into pseudoscalar pairs numerically, we take the elec-

tromagnetic coupling constant $\alpha = \frac{1}{137}$ and the QCD running coupling constant calculated to two-loop accuracy given by

$$\alpha_s(\mu_R^2) = \frac{4\pi}{\beta_0 \ln\left(\frac{\mu_R^2}{\Lambda_{QCD}^2}\right)} \left\{ 1 - \frac{\beta_1}{\beta_0^2} \frac{\ln\ln\left(\frac{\mu_R^2}{\Lambda_{QCD}^2}\right)}{\ln\left(\frac{\mu_R^2}{\Lambda_{QCD}^2}\right)} \right\} \quad (35)$$

with $\beta_0 = \frac{11N_c - 2N_f}{3}$ and $\beta_1 = \frac{34N_c^3 - 13N_c^2 N_f + 3N_f^2}{3N_c}$. The QCD scale is taken as $\Lambda_{QCD} \in (0.15, 0.3)$ GeV and the interaction scale is chosen as $\mu_R^2 = W^2$ in this work.

Next, we focus on the chiral enhancing scale μ_M , which is an important parameter with a significant influence to the contribution from twist-3 parts of the pseudoscalar meson in the $\gamma\gamma \rightarrow M^+ M^-$ process. According to its definition,

$$\mu_M = \frac{m_M^2}{m_q + m_{\bar{q}}}, \quad (M = \pi, K; q, \bar{q} = u, d, s), \quad (36)$$

and the one-loop expression for the running quark mass in the $\overline{\text{MS}}$ scheme [47] is

$$m(\mu_R^2) = m(\mu_0^2) \left(\frac{\alpha_s(\mu_R^2)}{\alpha_s(\mu_0^2)} \right)^{\frac{\gamma_m^{(0)}}{2\beta_0}} \quad (37)$$

with the anomalous dimension of the quark mass $\gamma_m^{(0)} = 6C_F$ and the β function $\beta_0 = \frac{11N_c - 2N_f}{3}$ as defined above, we

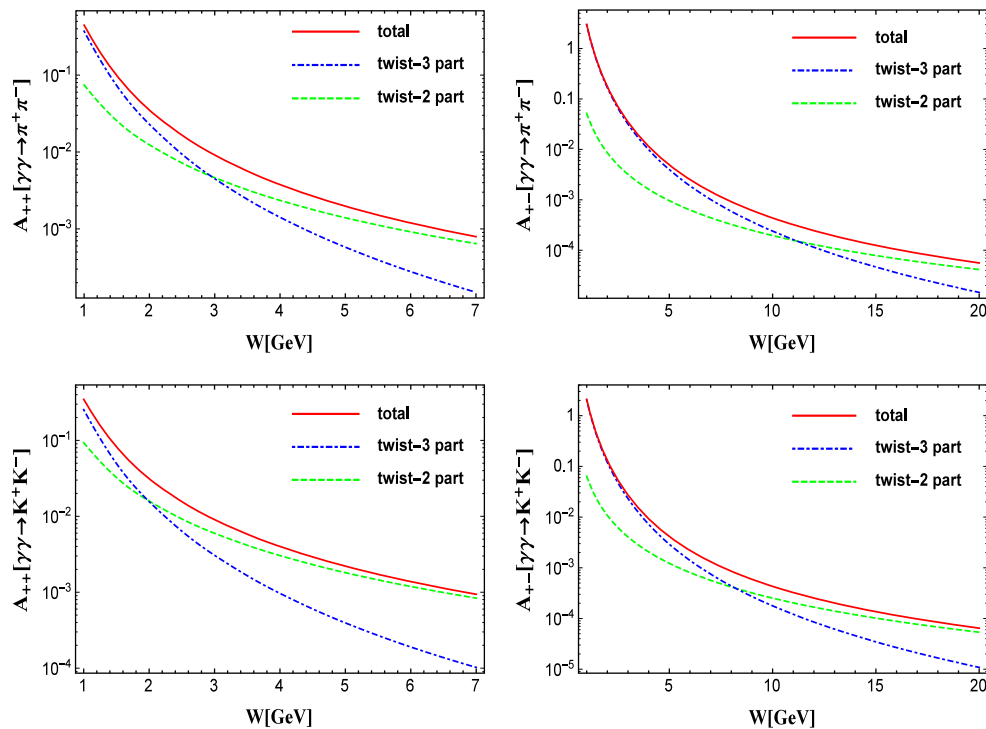


Fig. 3 Dependence of the prediction for $\gamma\gamma \rightarrow \bar{M}M$ transitional matrix element $A_{\lambda_1 \lambda_2}$ on the energy W with $\cos\theta = 0$ in the pion and kaon case, respectively

can get μ_π for the pion and μ_K for the kaon with the different energy scale $\mu_R^2 = W^2$. The masses of the current quarks are $m_\mu(1 \text{ GeV}) = m_d(1 \text{ GeV}) = 4 \text{ MeV}$ and $m_s(1 \text{ GeV}) = 140 \text{ MeV}$ [39]. The masses of the pseudoscalar mesons $m_\pi = 139.6 \text{ MeV}$ and $m_K = 493.7 \text{ MeV}$ are quoted from PDG [48]. With the help of Eqs. (36) and (37), we work out $2.44 \text{ GeV} \leq \mu_\pi \leq 3.66 \text{ GeV}$ and $1.69 \text{ GeV} \leq \mu_K \leq 2.55 \text{ GeV}$ in the energy scale $W \in (1, 6)$.

The transitional matrix elements $A_{\lambda_1 \lambda_2}$ of the two-pion and two-kaon processes are shown in Fig. 3 with the two-photon energy W as a variable parameter. Here we choose $\cos\theta = 0$ and a_n^i as the central value in Eq. (33) for the meson distribution amplitudes and $\Lambda_{QCD} = 0.2 \text{ GeV}$ for the strong coupling constant. Considering the polarization states of two photons, there are some relationships $A_{++} = A_{--}$ and $A_{+-} = A_{-+}$ in our calculation. In Fig. 3, the left two figures and the right two figures are the transitional matrix elements A_{++} and A_{+-} for the pion and kaon case, respectively. The green dashed curves are the contributions from twist-2 distribution amplitudes, the blue dot-dashed curves are contributions from twist-3 distribution amplitudes and the red solid curves are total contributions with twist-2 part and twist-3 part. Compared with the leading-twist contribution, we can see that the twist-3 contribution is suppressed in the transitional matrix element A_{++} as the energy $W > 3 \text{ GeV}$ (2 GeV) for the pion (kaon), while a similar

condition occurred in the transitional matrix element A_{+-} as the energy $W > 11 \text{ GeV}$ (8 GeV) for pion (kaon).

Integrating over the scattering angular with $|\cos\theta| < 0.6$, the cross sections $\sigma_0(\gamma\gamma \rightarrow \pi^+\pi^-)$ and $\sigma_0(\gamma\gamma \rightarrow K^+K^-)$ are shown in Fig. 4. The banded structures come from the twist-3 correction. It is important to note that the phrase twist-3 correction in the text and the legend twist-3 in the figure all mean the contribution including the total twist-2 part and twist-3 part in the following paragraphs. The green band denotes twist-3(a) with the variable a_n^i and α_s with $\Lambda_{QCD} \in (0.15, 0.3) \text{ GeV}$. The yellow band is for twist-3(b) with the variable a_n^i at $\Lambda_{QCD} = 0.2 \text{ GeV}$ for α_s . Here we can see that the strong coupling constant α_s has little effect at the lower limit but it has an obvious effect to the upper limit from the areas of two bands. The choice of distribution amplitudes has a significant influence on the cross section from the yellow band. The magenta solid line named twist-2 stands for the contribution from twist-2 part with $\Lambda_{QCD} = 0.2 \text{ GeV}$ for α_s and a_n^i chosen as the central value in Eq. (33). The experimental data from TPC [11], BELLE [14] and ALEPH [12] are also displayed simultaneously in Fig. 4 and we find that the twist-3 correction to the cross section is markedly improved, even more than an order of magnitude enhanced compared with the leading-twist contribution and the one-loop correction [18]. Especially, our results of the cross sections for the pion and kaon channels are in good agreement with the experimental data in the energy $W > 2.8 \text{ GeV}$.

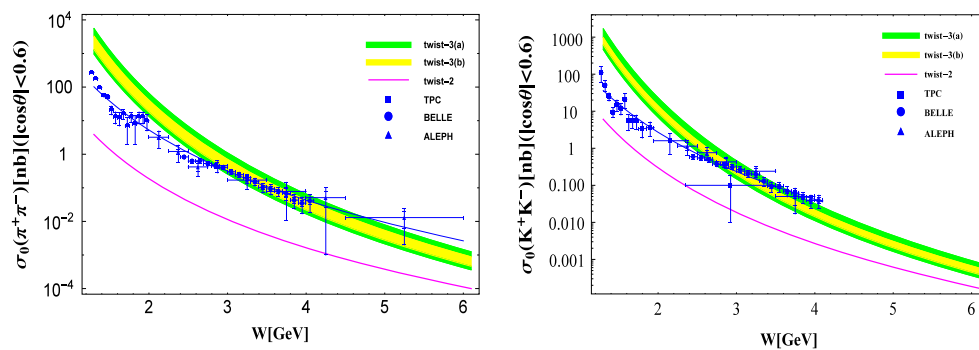


Fig. 4 Cross section for $\gamma\gamma \rightarrow \bar{M}M$ in the c.m. angular region $|\cos\theta| < 0.6$. The blue solid line is the result of a fit for the data among relevant ranges

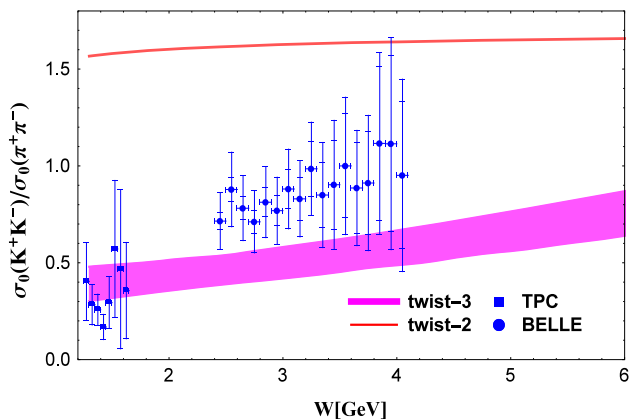


Fig. 5 Cross section ratio of $\gamma\gamma \rightarrow \pi^+\pi^-$ to $\gamma\gamma \rightarrow K^+K^-$. The experimental points are from TPC [11] and BELLE [14]

Our curves differ significantly from the predictions made before due to considering the contributions from twist-3 parts. We know the parametrization about the W dependence of the cross section, which has the form of $\sigma(\gamma\gamma \rightarrow M^+M^-) \propto W^{-n_M}$. In Ref. [14], the BELLE Collaboration announce that they find $n_\pi = 7.9 \pm 0.4 \pm 1.5$ and $n_K = 7.3 \pm 0.3 \pm 1.5$ for $3.0 \text{ GeV} < W < 4.1 \text{ GeV}$. In Ref. [18], the NLO results give the power $n_\pi = n_K = 6.9(7.4)$ for $\mu_R^2 = W^2(W^2/15)$. On the other hand, we carry out a simple theoretic fitting for the experimental data, which are mentioned in Fig. 4 among $1.25 \text{ GeV} < W < 6(4.1) \text{ GeV}$ for pion (kaon), and we obtain $n_\pi = 6.91$ and $n_K = 6.02$ corresponding to the blue solid curves in Fig. 4. At the same time, we find that the powers are $n_\pi = 6.76$ and $n_K = 6.73$ from our twist-2 contributions and the powers are $n_\pi = 9.63$ and $n_K = 9.20$ from our twist-3 correction. The analysis of the powers shows that our predictions from twist-3 correction change faster than the experimental data but their values are of similar magnitude to the data from BELLE, ALEPH, TPC, and vice versa for twist-2 parts.

The ratio K^+K^- to $\pi^+\pi^-$ is showed in Fig. 5. The experimental points are calculated from the data of TPC

[11] with the energy $W \in (1.2, 2.0) \text{ GeV}$ and BELLE [14] with the energy $W \in (2.4, 4.1) \text{ GeV}$. The red solid curve is the contribution of the twist-2 distribution amplitude from the first three terms Gegenbauer polynomials with the $\Lambda_{QCD} = 0.2$ and a_n^i taken as the center value of Eq. (33) and it is larger than the experimental data. The prediction in Ref. [6] approximately equals 1.06 and the one-loop prediction $f_K^4/f_\pi^4 = 2.23$ [18] coincides with the BL estimate [5] with the asymptotic leading-twist distribution amplitude, while the Belle measured value is $0.89 \pm 0.04 \pm 0.15$ in the energy $W \in (3.0, 4.1) \text{ GeV}$. The magenta band is from our twist-3 correction with the variable a_n^i and α_s with $\Lambda_{QCD} \in (0.15, 0.3) \text{ GeV}$ and it is in agreement with the experimental data.

In Fig. 6, we display the angular dependence of cross section, $\sigma_0^{-1} d\sigma/d|\cos\theta|$ for the $\pi^+\pi^-$ and K^+K^- processes, respectively. There is no obvious change to our prediction for the ratio by varying W from 2.4 to 4.1, where the Belle data [14] are covered. To simplify our analysis, we only discuss our prediction and the Belle data at the $W = 3.2 \sim 3.3 \text{ GeV}$ region. The discrete points come from the experimental data in the angular region $|\cos\theta| \leq 0.6$. The dotted curves indicate the expectation from the $\sin^{-4}\theta$ behavior predicted by Brodsky and Lepage [5]. The dot-dashed and solid curves correspond to the twist-2 contribution and twist-3 correction in the angular $|\cos\theta| \leq 0.7$, respectively. One in particular is to expand the scattering angle to $|\cos\theta| \leq 0.7$ in our drawing and it is aimed at reflecting the distinction between twist-2 contribution and twist-3 correction. It is no problem, because the deviation of $\sigma_0^{-1} d\sigma/d|\cos\theta|$ from the different cut-off $|\cos\theta| \leq 0.6$ and $|\cos\theta| \leq 0.7$ is less than 5%. In Fig. 6, we can see that our theoretical predictions are compatible with the experimental data. When we take $|\cos\theta| \leq 0.6$, the curves from the twist-2 contribution and the twist-3 correction have similar changes with $\sin^{-4}\theta$. But as we take $|\cos\theta| > 0.6$, the curves from the twist-3 correction rapidly increase.

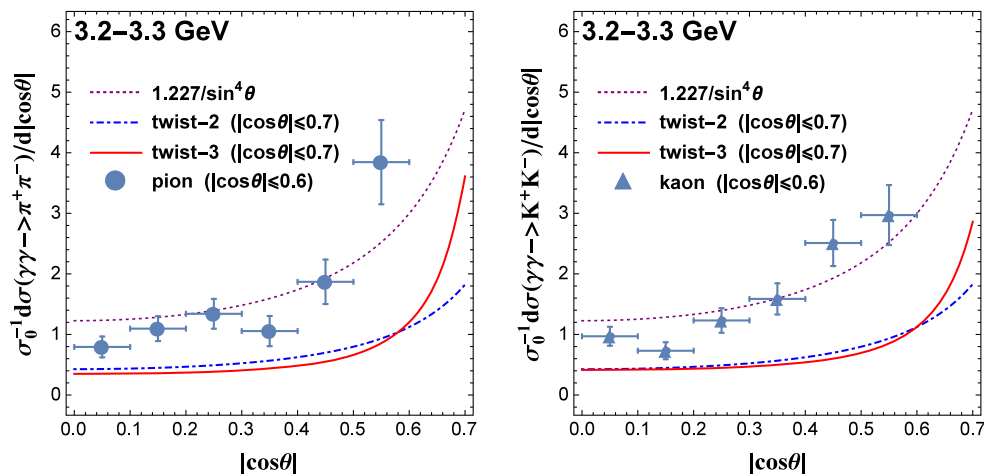


Fig. 6 Angular dependence of the cross section, $\sigma_0^{-1} d\sigma/d|\cos\theta|$ for $\pi^+\pi^-$, K^+K^- . The experimental points are from the Belle Collaboration [14]

5 Conclusion

In this work, we recalculate the processes of two-photon annihilation into two pseudoscalar mesons with the corrections of the two-particle twist-3 distribution amplitudes of pseudoscalar mesons in the standard hard-scattering approach. In order to avoid the endpoint singularity from twist-3 distribution amplitudes, we take distribution amplitudes of the meson with the BHL prescription. The twist-3 corrections of cross sections for $\gamma\gamma \rightarrow \pi^+\pi^-$, K^+K^- are markedly improved, even more than an order of magnitude enhanced compared with the twist-2 contributions. The results show that the contributions from twist-3 parts are actually not power suppressed compared with the leading-twist contributions, because momentum transfer is not large enough in those processes. The cross sections with twist-3 corrections have similar changes and are at the same order in magnitude with the data by varying the center-of-mass energy W from 1 to 6 GeV. We also discuss the cross section ratio $\sigma_0(K^+K^-)/\sigma_0(\pi^+\pi^-)$ and find it to be close to experimental results. Numerical analysis of the angular dependence of $\sigma_0^{-1} d\sigma/d|\cos\theta|$ shows that the ratios are independent of the distribution amplitudes and are in good agreement with the experimental data in the small-angle area, but the ratios with the twist-3 corrections increase faster than the ones from the twist-2 parts in the large-angle area.

Acknowledgements We gratefully acknowledge many helpful discussions with F. G. Cao, H. Q. Zhou, W. L. Sang and L. Cao. This work was supported by the Natural Science Foundation of China, Grant Number 11005087, 11175146 and 11645002, the Fundamental Research Funds for the Central Universities, Grant Number XDJK2014C169, XDJK2016C067, the Natural Science Foundation of ChongQing, Grant Number cstc2014jcyjA00029, the Open Project Program of State Key Laboratory of Theoretical Physics, Grant Number Y4KF081CJ1.

Open Access This article is distributed under the terms of the Creative Commons Attribution 4.0 International License (<http://creativecommons.org/licenses/by/4.0/>), which permits unrestricted use, distribution, and reproduction in any medium, provided you give appropriate credit to the original author(s) and the source, provide a link to the Creative Commons license, and indicate if changes were made. Funded by SCOAP³.

Appendix A: The expression of hard-scattering amplitudes $T_{\lambda_1\lambda_2}^{ij}(x, y, W, \theta)$

In this appendix, we present the detailed formulas of hard-scattering amplitudes $T_{\lambda_1\lambda_2}^{ij}(x, y, W, \theta)$ with the contributions from the two-particle twist-2 and twist-3 distribution amplitudes in the $\gamma\gamma \rightarrow \pi^+\pi^-$ process and the relevant expressions for the $\gamma\gamma \rightarrow K^+K^-$ process can be obtained by making the replacements of $f_\pi \rightarrow f_K$, $\mu_\pi \rightarrow \mu_K$ and $e_d \rightarrow e_s$ in the following formulas.

The leading-twist hard-scattering amplitudes for the $\pi^+\pi^-$ channel are expressed as

$$\begin{aligned}
 T_{++}^{\pi\pi} &= T_{--}^{\pi\pi} \\
 &= \frac{16\pi^2 \alpha_s(\mu_R^2) C_F f_\pi^2 [-y + x(-1 + 2y)](e_d - e_u)^2}{3(-1 + t^2)W^2(-1 + x)x(-1 + y)y}, \\
 T_{+-}^{\pi\pi} &= T_{-+}^{\pi\pi} = \frac{4\pi^2 \alpha_s(\mu_R^2) C_F f_\pi^2}{3(-1 + t^2)W^2(-1 + x)x(-1 + y)y} \\
 &\times \left\{ 2[-1 + x + y - 4xy + t^2(-1 + x + y)]e_d^2 \right. \\
 &+ \frac{1}{[x(1 + t - 2y) + y - ty][-(1 + t)y + x(-1 + t + 2y)]} \\
 &\times \{ 4[-(-1 + t^2)(-1 + y)y^2 \\
 &+ x^3(-1 + 2y)(-1 + t^2 + 8y - 8y^2) \\
 &+ x^2[-1 + 11y - 32y^2 + 24y^3 + t^2(1 + 5y - 8y^2)] \}
 \end{aligned}$$

$$+xy[-2+11y-10y^2+t^2(-6+5y+2y^2)]e_de_u\} \\ -[6-6y+2t^2(-1+x+y)+x(-6+8y)]e_u^2\},$$

where α and α_s mean the electromagnetic coupling constant and the strong coupling constant, respectively. The variables x and y are the momentum fractions from the final pseudoscalar mesons. The quark charges are $e_u = \frac{2}{3}$ for the u quark and $e_{d(s)} = -\frac{1}{3}$ for the $d(s)$ quark. The color factor is $C_F = \frac{N_C^2-1}{2N_C}$ with the color number $N_C = 3$. If we make the replacement of $t \rightarrow \cos \theta$ in the above expression, we reduce them to new formulas that have the same forms as the theoretical prediction of Chernyak [9, 10], Brodsky [5] and Nizic [17] on the leading-twist order.

It is convenient to take $\cos \theta$ as t in the numerical analysis of the twist-3 parts and the twist-3 hard-scattering amplitudes are represented as follows:

$$T_{++}^{pp} = T_{--}^{pp} = -\frac{8\pi^2\alpha\alpha_s(\mu_R^2)C_F f_\pi^2 \mu_\pi^2}{3(-1+t^2)W^4(-1+x)x(-1+y)y} \\ \times \left\{ -2\{2y+x[2+(-3+t^2)y]\}e_d^2 \right. \\ + \frac{1}{[x(1+t-2y)+y-ty][-(1+t)y+x(-1+t+2y)]} \\ \times \{8(-1+t^2)(-1+y)y^2 \\ + x^3(-1+2y)[1-y+y^2+t^2(-1-y+y^2)] \\ + xy[2-4y+3y^2-t^2(-2+2y+y^2)] \\ - x^2[-1+4y-4y^2+3y^3+t^2(1+2y-8y^2+3y^3)]\}e_de_u \\ \left. - 2[1+x+t^2(-1+x)(-1+y)+y-3xy]e_u^2 \right\}, \\ T_{+-}^{pp} = T_{-+}^{pp} = \frac{8\pi^2\alpha\alpha_s(\mu_R^2)C_F f_\pi^2 \mu_\pi^2}{3(1-t^2)W^4} \\ \times \left\{ \frac{2[-1+x(2-3y)+2y+t^2(-1+xy)]e_d^2}{(-1+x)^2(-1+y)^2} \right. \\ - \frac{8(1+t^2)[-y+x(-1+2y)]e_de_u}{[x(1+t-2y)+y-ty][-(1+t)y+x(-1+t+2y)]} \\ + \frac{2[x+[1+t^2(-1+y)-3y]+y-t^2y]e_u^2}{x^2y^2} \left. \right\}, \\ T_{++}^{p\sigma} = T_{--}^{p\sigma} = -\frac{16\pi^2\alpha\alpha_s(\mu_R^2)C_F f_\pi^2 \mu_\pi^2}{9(-1+t^2)^2W^4(-1+x)^2x^2} \\ \times \left\{ -\frac{(-1+t^2)(-1+x)(1+t^2x)e_d^2}{-1+y} \right. \\ + \frac{1}{(-1+y)y[-x(1+t-2y)+(-1+t)y](x-tx+y+ty-2xy)} \\ \times \{2(-1+t^2)(-1+y)y^2 \\ + xy[-1+y+2t^2y-2y^2+t^4(1-3y+2y^2)] \\ + x^5[1-4y+6y^2-4y^3+t^4(-1+2y)-6t^2y(1-3y+2y^2)] \\ + x^2y[-3+8y+2y^2+t^4(1+10y-12y^2)+2t^2(1-13y+9y^2)] \\ + x^3[-1+6y-6y^2-8y^3+t^2(2-6y+42y^2-32y^3)] \\ + t^4(-1-8y+4y^2+8y^3)] \\ + x^4[t^4(2+3y-8y^2)+y(1-6y+10y^2) \\ + 2t^2(-1+6y-21y^2+15y^3)]\}e_de_u\}$$

$$+ \frac{(-1+t^2)[-1+t^2(-1+x)]xe_u^2}{y} \left. \right\}, \\ T_{+-}^{p\sigma} = T_{-+}^{p\sigma} = -\frac{8\pi^2\alpha\alpha_s(\mu_R^2)C_F f_\pi^2 \mu_\pi^2}{9(-1+t^2)^2W^4(-1+x)^3x^3} \\ \times \left\{ \frac{(-1+t^2)x^2[-1+2x+t^2(-1-2x+2x^2)]e_d^2}{-1+y} \right. \\ + \frac{1}{(-1+y)y[x(1+t-2y)+y-ty][-(1+t)y+x(-1+t+2y)]} \\ \times \{4(-1+x)^2x^2\{-(-1+t^2)y^2[-1+2y+t^2(-3+4y)] \\ + x^3[1-4y+6y^2-4y^3+t^4(-1+2y)-6t^2y(1-3y+2y^2)] \\ + xy[-1+4y-6y^2+t^2(2+8y-10y^2)+t^4(-1-4y+8y^2)] \\ + x^2y[1+t^4(5-8y)-4y+6y^2+2t^2(1-10y+9y^2)]\}e_de_u \\ + \frac{(-1+t^2)(-1+x)^2[1-2x+t^2(-1-2x+2x^2)]e_u^2}{y} \left. \right\}, \\ T_{++}^{\sigma p} = T_{--}^{\sigma p} = -\frac{16\pi^2\alpha\alpha_s(\mu_R^2)C_F f_\pi^2 \mu_\pi^2}{9(-1+t^2)^2W^4(-1+y)^2y^2} \\ \times \left\{ -\frac{(-1+t^2)(-1+y)(1+t^2y)e_d^2}{-1+x} \right. \\ + \frac{1}{(-1+x)x[x(1+t-2y)+y-ty][-(1+t)y+x(-1+t+2y)]} \\ \times \{2(-1+t^2)(-1+y)y^3[1+t^2(-1+y)+y] \\ + xy[-1-3y+6y^2+y^3-4y^4] \\ + 2t^2y(1-3y+6y^2-3y^3)+t^4(1+y-8y^2 \\ + 3y^3+2y^4)]-x^3(-1+2y) \\ \times [1+2y^2-4y^3+2y^4+t^4(1+4y-4y^2) \\ + 2t^2(-1-2y+5y^2-6y^3+3y^4)] \\ + x^2[-1+y+8y^2-6y^3-6y^4+6y^5 \\ + t^4(-1-3y+10y^2+4y^3-8y^4) \\ + 2t^2(1+y-13y^2+21y^3-21y^4+9y^5)]\}e_de_u \\ + \frac{(-1+t^2)[-1+t^2(-1+y)]ye_u^2}{x} \left. \right\}, \\ T_{+-}^{\sigma p} = T_{-+}^{\sigma p} = -\frac{8\pi^2\alpha\alpha_s(\mu_R^2)C_F f_\pi^2 \mu_\pi^2}{9(-1+t^2)^2W^4(-1+y)^3y^3} \\ \times \left\{ \frac{(-1+t^2)y^2[-1+2y+t^2(-1-2y+2y^2)]e_d^2}{-1+x} \right. \\ + \frac{1}{(-1+x)x[x(1+t-2y)+y-ty][-(1+t)y+x(-1+t+2y)]} \\ \times \{4(-1+y)^2y^2\{-(-1+t^4)y^3 \\ + xy[-1+y-4y^2+t^2(2+2y-6y^2) \\ + t^4(-1+5y+2y^2)]+2x^3[1-3y+3y^2-2y^3] \\ + t^4(-2+4y)+t^2(1-5y+9y^2-6y^3)] \\ + x^2[-1+4y-4y^2+6y^3+t^4(3-4y-8y^2) \\ + 2t^2(-1+4y-10y^2+9y^3)]\}e_de_u \\ + \frac{(-1+t^2)(-1+y)^2[1-2y+t^2(-1-2y+2y^2)]ye_u^2}{x} \left. \right\}, \\ T_{++}^{\sigma\sigma} = T_{--}^{\sigma\sigma} = \frac{2\pi^2\alpha\alpha_s(\mu_R^2)C_F f_\pi^2 \mu_\pi^2}{27(1-t^2)^2W^4} \\ \times \left\{ \frac{2(1+t^2)[x(-1+y)-y]e_d^2}{(-1+x)^2x(-1+y)^2y} + (-1+t^2)^2 \right. \\ \times \left\{ -\frac{1}{(1+t)^4x^2(-1+y)^2[x(1+t-2y)+y-ty]^2} \right. \\ \left. \left. \right\} \right\}$$

$$\begin{aligned}
& \times \{4\{-(-1+t)[-1+t(-1+y)-y](-1+y)y \\
& + x^3[-1+4y-6y^2+4y^3 \\
& + t^2(-1+2y)+t(-2+6y-6y^2)] \\
& + x[2-2y-2y^2+4y^3-t^3(-1+y^2) \\
& + t(5-4y+3y^2-6y^3)+2t^2(2-y-2y^2+y^3)] \\
& + x^2[-1+t^3(-1+y) \\
& + 4y^2-6y^3+t^2(-3+6y-4y^2)+t(-3+5y-4y^2+6y^3)]\} \\
& + \frac{1}{(-1+t)^4 x^2(-1+y)^2(x-tx+y+ty-2xy)^2} \\
& \times \{4\{(1+t)(-1+y)y[1+t(-1+y)+y] \\
& + x^3[1+t^2(1-2y)-4y+6y^2-4y^3 \\
& + t(-2+6y-6y^2)]+x[-t^3(-1+y^2) \\
& + t(5-4y+3y^2-6y^3)+2(-1+y+y^2-2y^3) \\
& -2t^2(2-y-2y^2+y^3)] \\
& + x^2[1+t^3(-1+y)-4y^2+6y^3+t^2(3-6y+4y^2) \\
& + t(-3+5y-4y^2+6y^3)]\} \\
& - \frac{1}{(-1+t)^4(-1+x)^2 y^2[x(1+t-2y)+y-ty]^2} \\
& \times \{4\{(-1+t)^2(-2+t-y)(-1+y)y \\
& + x^3[-1+4y-6y^2+4y^3+t^2(-1+2y)+t(-2+6y-6y^2)] \\
& -(-1+t)x[1-2y+t^2 y^2+4y^3+t(1+2y-5y^2-2y^3)] \\
& + x^2[t^3 y+t^2(2-4y-4y^2)-2y(1-2y+3y^2) \\
& + t(2-3y+4y^2+6y^3)]\} \\
& + \frac{1}{(1+t)^4(-1+x)^2 y^2(x-tx+y+ty-2xy)^2} \\
& \times \{4\{(1+t)^2(-1+y)y(2+t+y) \\
& + x^3[1+t^2(1-2y)-4y+6y^2-4y^3+t(-2+6y-6y^2)] \\
& - (1+t)x[1-2y+t^2 y^2+4y^3+t(-1-2y+5y^2+2y^3)] \\
& + x^2[t^3 y+2y(1-2y+3y^2)+t^2(-2+4y+4y^2) \\
& + t(2-3y+4y^2+6y^3)]\} \\
& + \frac{2(1+t^2)(-1+xy)e_u^2}{(-1+x)x^2(-1+y)y^2} \Big\} e_d e_u \\
& + \frac{2(1+t^2)(-1+xy)e_u^2}{(-1+x)x^2(-1+y)y^2} \Big\} \\
T_{+-}^{\sigma\sigma} = T_{-+}^{\sigma\sigma} = & \frac{4\pi^2 \alpha_s (\mu_R^2) C_F f_\pi^2 \mu_\pi^2}{27(-1+t^2)W^4} \\
& \times \left\{ \frac{(1+t^2)[2+x(-1+y)-y]e_d^2}{(-1+x)^2 x(-1+y)^2 y} - \frac{1}{(-1+t^2)^2} \right. \\
& \times 2 \left\{ \frac{1}{x^2(-1+y)^2[x(-1+t-2y)+y-ty]^2}(-1+t)^4 \right. \\
& \times \{1(-1+t)[-3+t(-1+y)-y]y^2 \\
& + x^3[-1+4y-6y^2+4y^3+t^2(-1+2y) \\
& + t(-2+6y-6y^2)]+x^2[-2+t^3(-1+y) \\
& + 6y-4y^2-6y^3+t^2(-4+6y-4y^2) \\
& + t(-5+11y-4y^2+6y^3)]+x[1-4y \\
& + 8y^2+4y^3-t^3(-1+y^2)+t^2(3-4y^2+2y^3) \\
& - t(-3+4y+3y^2+6y^3)]\} \\
& - \frac{1}{x^2(-1+y)^2(x-tx+y+ty-2xy)^2}(-1+t)^4 \\
& \times \{(1+t)y^2[3+t(-1+y)+y] \\
& + x^3[1+t^2(1-2y)-4y+6y^2-4y^3 \\
& + t(-2+6y-6y^2)]+x^2[2+t^3(-1+y)
\end{aligned}$$

$$\begin{aligned}
& -6y+4y^2+6y^3+t^2(4-6y+4y^2) \\
& + t(-5+11y-4y^2+6y^3)]-x[1-4y \\
& + 8y^2+4y^3+t^3(-1+y^2)+t^2(3-4y^2+2y^3) \\
& + t(-3+4y+3y^2+6y^3)]\} \\
& + \frac{1}{(-1+x)^2 y^2[x(1+t-2y)+y-ty]^2}(-1+t)^4 \\
& \times \{(-1+t)^2 y[1+t(-1+y)-2y-y^2] \\
& -(-1+t)xy[-4+(6-5t+t^2)y-2(-2+t)y^2] \\
& + x^3[-1+4y-6y^2+4y^3+t^2(-1+2y)+t(-2+6y-6y^2)] \\
& + x^2[-3+8y+t^3 y-4y^2-6y^3+t^2(1-4y-4y^2) \\
& + t(-2+3y+4y^2+6y^3)]\} \\
& - \frac{1}{(-1+x)^2 y^2(x-tx+y+ty-2xy)^2}(-1+t)^4 \\
& \times \{(1+t)^2 y[-1+t(-1+y)+2y+y^2] \\
& - (1+t)xy[-4+(6-5t+t^2)y+2(2+t)y^2] \\
& + x^3[1+t^2(1-2y)-4y+6y^2-4y^3+t(-2+6y-6y^2)] \\
& + x^2[3-8y+t^3 y+4y^2+6y^3+t^2(-1+4y+4y^2) \\
& + t(-2+3y+4y^2+6y^3)]\} \\
& + \frac{(1+t^2)(1+xy)e_u^2}{(-1+x)x^2(-1+y)y^2} \Big\} e_d e_u \\
& + \frac{(1+t^2)(1+xy)e_u^2}{(-1+x)x^2(-1+y)y^2} \Big\} .
\end{aligned}$$

References

- V.L. Chernyak, A.R. Zhitnitsky, JETP Lett. **25**, 510 (1977)
- V.L. Chernyak, A.R. Zhitnitsky, V.G. Serbo, JETP Lett. **26**, 594 (1977)
- V.L. Chernyak, A.R. Zhitnitsky, Phys. Rep. **112**, 173 (1984)
- G. Peter Lepage, S.J. Brodsky, Phys. Rev. D **22**, 2157 (1980)
- S.J. Brodsky, G. Peter Lepage, Phys. Rev. D **24**, 1808 (1981)
- M. Benayoun, V.L. Chernyak, Nucl. Phys. B **329**, 285 (1990)
- S.J. Brodsky, Invited talk presented at Photon 2000, Ambleside, England, August 26–31 (2000). [arXiv:hep-ph/0010176v1](https://arxiv.org/abs/hep-ph/0010176v1)
- S.J. Brodsky, Invited talk presented at Photon 2005, Warsaw, Poland, 30 August–8 September (2005)
- V.L. Chernyak, Nucl. Phys. B (Proc. Suppl.) **162**, 161 (2006). [arXiv:hep-ph/0605327v2](https://arxiv.org/abs/hep-ph/0605327v2)
- V.L. Chernyak, S.I. Eidelman, Prog. Part. Nucl. Phys. **80**, 1 (2015). [arXiv:hep-ph/1409.3348v2](https://arxiv.org/abs/hep-ph/1409.3348v2)
- H. Aihara et al. (TPC/Two-Gamma Collaboration), Phys. Rev. Lett. **57**, 404 (1986)
- A. Heister et al. (ALEPH Collaboration), Phys. Lett. B **569**, 140 (2003)
- K. Abe et al. (Belle Collaboration), Eur. Phys. J. C **32**, 323 (2004)
- H. Nakazawa et al. (Belle Collaboration), Phys. Lett. B **615**, 39 (2005). <http://durpdg.dur.ac.uk/view/6084192>
- H. Nakazawa (Belle Collaboration), Nucl. Part. Phys. Proc. **260**, 98 (2015)
- T. Mori et al. (Belle Collaboration), J. Phys. Soc. Jpn. **76**, 074102 (2007)
- B. Nižić, Phys. Rev. D **35**, 80 (1987)
- G. Duplancić, B. Nižić, Phys. Rev. Lett. **97**, 142003 (2006)
- M.-Z. Zhou, H.-Q. Zhou, Phys. Rev. D **80**, 094021 (2009)
- X.-G. Wu, T. Huang, J. High Energy Phys. **04**, 043 (2008)
- X.-G. Wu, T. Huang, Int. J. Mod. Phys. A **21**, 901 (2006). [arXiv:hep-ph/0507136](https://arxiv.org/abs/hep-ph/0507136)
- L.-B. Chen, C.-F. Qiao, J. High Energy Phys. **11**, 168 (2012)
- I.V. Anikin, D.Yu. Ivanov, B. Pire, L. Szymanowski, S. Wallon, Nucl. Phys. B **828**, 1 (2010)

24. I.V. Anikin, D.Yu. Ivanov, B. Pire, L. Szymanowski, S. Wallon, Phys. Lett. B **682**, 413 (2010)
25. V.M. Braun, I.B. Filyanov, Z. Phys. C **48**, 239 (1990)
26. P. Ball, J. High Energy Phys. **01**, 010 (1999). [arXiv:hep-ph/9812375v1](https://arxiv.org/abs/hep-ph/9812375v1)
27. R. Jakob, P. Kroll, Phys. Lett. B **315**, 463 (1993)
28. T. Huang, X.-G. Wu, Phys. Rev. D **70**, 093013 (2004)
29. S.J. Brodsky, T. Huang, G.P. Lepage, in *Particles and Fields-2, Proceedings of the Banff Summer Institute, Banff, Alberta, 1981*, ed. by A.Z. Capri, A.N. Kamal (Plenum, New York, 1983), p. 143
30. G.P. Lepage, S.J. Brodsky, T. Huang, P.B. Mackenzie, in *Particles and Fields-2, Proceedings of the Banff Summer Institute, Banff, Alberta, 1981*, ed. by A.Z. Capri, A.N. Kamal (Plenum, New York, 1983), p. 83
31. T. Huang, B.-Q. Ma, Q.-X. Shen, Phys. Rev. D **49**, 1490 (1994)
32. V.M. Braun, I.E. Filyanov, Z. Phys. C **44**, 157 (1989)
33. M. Nagashima, H. Li, Eur. Phys. J. C. **40**, 395 (2005)
34. M. Beneke, T. Feldmann, Nucl. Phys. B **592**, 3 (2001)
35. H.C. Pauli, Eur. Phys. J. C **7**, 289 (1999)
36. S.J. Brodsky, G.F. de Tramondb, H.G. Doschc, J. Erlich, Phys. Rep. **584**, 1 (2015)
37. A. Vega, I. Schmidt, T. Branz, T. Gutsche, V.E. Lyubovitskij, Phys. Rev. D **80**, 055014 (2009)
38. R. Swarnkar, D. Chakrabarti, Phys. Rev. D **92**, 074023 (2015)
39. P. Ball, V.M. Braun, A. Lenz, J. High Energy Phys. **05**, 004 (2006). [arXiv:hep-ph/0603063v1](https://arxiv.org/abs/hep-ph/0603063v1)
40. T. Huang, M.-Z. Zhou, X.-G. Wu, Eur. Phys. J. C **42**, 271 (2005)
41. V.L. Chernyak, A.R. Zhitnitsky, Nucl. Phys. B **201**, 492 (1982)
42. V.M. Braun et al., Phys. Rev. D **74**, 074501 (2006)
43. R. Arthur et al., Phys. Rev. D **83**, 074505 (2011)
44. V.M. Braun et al., Phys. Rev. D **92**, 014504 (2015)
45. T. Huang, X.G. Wu, Int. J. Mod. Phys. A **22**, 3065 (2007)
46. T. Huang, T. Zhong, X.-G. Wu, Phys. Rev. D **88**, 034013 (2013)
47. A.J. Buras, in *Les Houches Summer School in Theoretical Physics Conference: C97-07-28*, p. 281–539. [arXiv:hep-ph/9806471v1](https://arxiv.org/abs/hep-ph/9806471v1)
48. K.A. Olive et al. (Particle Data Group), Chin. Phys. C **38**, 090001 (2014)